

## INVESTIGATING TENSILE STRENGTH IN SLA 3D PRINTING ENHANCEMENT THROUGH EXPERIMENTATION AND FINITE ELEMENT ANALYSIS

Siwasit Pitjamt<sup>1</sup>, Norrapon Vichiansan<sup>2\*</sup>, Parida Jewpanya<sup>3</sup>, Pinit Nuangpirom<sup>4</sup>, Pakpoom Jaichompoo<sup>5</sup>, Komgrit Leksakul<sup>6</sup>, Pattarawadee Poolperm<sup>7</sup>

Department of Industrial Engineering, Faculty of Engineering, Rajamangala University of Technology Lanna Tak, Tak 63000 Thailand<sup>135</sup>

Multidisciplinary Center, Faculty of Engineering, Chiang Mai University, Chiang Mai, 50200, Thailand<sup>2</sup>

Department of Electrical Engineering, Faculty of Engineering, Rajamangala University of Technology Lanna, Chiang Mai, 50300 Thailand<sup>4</sup>

Department of Industrial Engineering, Faculty of Engineering, Chiang Mai University, Chiang Mai 50200, Thailand<sup>6</sup>

Industrial Engineering Program, School of Engineering, Sripatum University, Bangkok, 10900, Thailand<sup>7</sup>

norrapon.v@cmu.ac.th<sup>2</sup>

Received: 20 May 2024, Revised: 11 August 2024, Accepted: 18 August 2024

\*Corresponding Author

### ABSTRACT

*This study aims to optimize tensile strength in Stereolithography (SLA) 3D printing by investigating the effects of print orientation and layer orientation on mechanical properties. Employing a multilevel factorial design, we systematically analyzed various print and layer orientations using both experimental and computational methods. The experimental component, performed with an Instron 5566 machine, identified a print orientation of 22.5 degrees and side orientations as optimal, achieving a tensile strength of 72.01 MPa. Computational simulations using ANSYS software supported these findings, showing a close correlation between experimental and simulated results. This research not only advances theoretical understanding of SLA 3D printing processes but also offers practical insights for optimizing tensile strength in manufacturing applications. By integrating experimental and finite element analysis (FEA) results, which predicted a maximum stress of 71.97 MPa under a 686 N load, the study contributes valuable knowledge for enhancing additive manufacturing practices and informs future research on parameter optimization.*

**Keywords :** SLA 3D Printing, Tensile Strength, Printing Process Parameters, Finite Element Analysis.

### 1. Introduction

Additive manufacturing, notably three-dimensional (3D) printing, has revolutionized the manufacturing industry by enabling the creation of complex and customized components from digital designs. This technology contrasts sharply with traditional subtractive methods that involve removing material from a solid block. By building objects layer by layer, 3D printing offers unparalleled design flexibility, rapid prototyping, and on-demand production, which have transformed various sectors including aerospace, medical, and automotive industries (Zhou & Wang, 2023; Rose & Bharadwaj, 2023). The ability to produce intricate geometries and tailor-made parts with ease underscores the disruptive nature of this technology (Doungkeaw et al., 2023; Tariq et al., 2023).

Despite its advancements, the quality and performance of 3D-printed components are significantly influenced by several factors, including material properties, printing parameters, and post-processing techniques. One critical aspect that affects mechanical properties and structural integrity is print orientation how the object is aligned relative to the build platform during printing (Dzogbewu et al., 2020; Nazir et al., 2023). However, determining the optimal print orientation remains challenging due to its interaction with part geometry, material characteristics, and application requirements (Marşavina et al., 2022; Jirků et al., 2023). This study addresses a notable gap in the literature regarding the systematic exploration of how print orientation angles affect the mechanical properties of 3D-printed materials. This gap is

significant as it influences both the performance of the final product and the efficiency of the manufacturing process. In industries where reliability and strength are crucial, such as aerospace and medical applications, an incomplete understanding of print orientation can lead to suboptimal designs and potential failures (Sossou et al., 2018; Kafle et al., 2021).

Previous research has explored various aspects of additive manufacturing, including material selection and process optimization (Fayazfar et al., 2018; Arefin et al., 2021; Ngo et al., 2018). However, while studies such as those by Caminero et al. (2019), Subbiah (2020), Fernández-Vicente et al. (2016), and Lalegan et al. (2020) have highlighted the impact of print orientation on mechanical properties, they have often focused on materials and processes different from SLA technology. This study aims to bridge this gap by examining the influence of varying print orientation angles specifically within SLA 3D printing contexts. Additionally, by integrating finite element analysis (FEA), the research introduces a novel approach to predicting tensile load capacity, thus extending previous findings and providing a more comprehensive understanding of SLA-printed materials. This approach contrasts with but complements existing studies by enhancing the accuracy of structural behavior predictions.

The primary objective of this study is to systematically investigate the effect of layer orientations on the mechanical properties of SLA-manufactured polymer materials. Utilizing a multilevel factorial design, the study will explore five orientation angles ( $0^\circ$ ,  $22.5^\circ$ ,  $45^\circ$ ,  $67.5^\circ$ , and  $90^\circ$ ) and two print orientations (flat and side) to provide insights into optimizing tensile strength and structural integrity. The findings aim to address challenges related to achieving consistent mechanical performance in 3D-printed components, particularly in high-reliability applications. Furthermore, the study will contribute to existing methodologies by offering a validated framework for using FEA to predict tensile load capacity, thereby improving design and manufacturing processes (Asif et al., 2019). The research framework is illustrated in Figure 1.

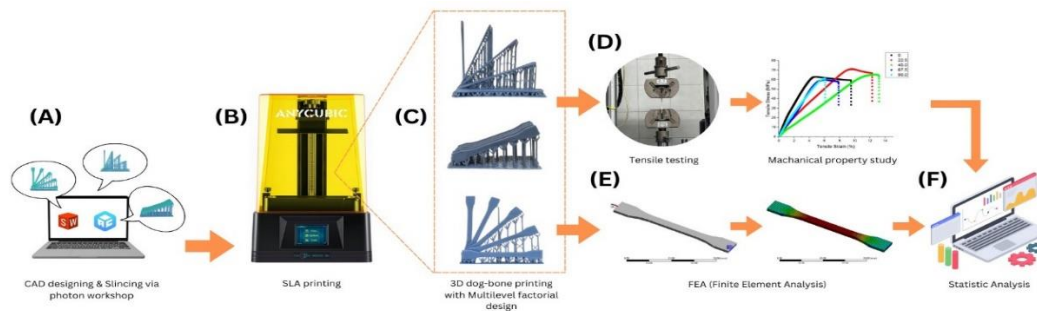


Fig. 1. The research framework of investigating tensile strength for SLA 3D Printing.

## 2. Material and methods

### 2.1 Tensile Testing Procedures

Tensile testing was conducted in strict accordance with the protocols specified in ISO 527, ensuring that the procedures followed are well-established and standardized for evaluating the tensile properties of plastic materials. For this study, Type 1BA specimens were selected as per the standard's guidelines, providing consistency in the testing process and enabling reliable comparisons of the mechanical properties across different print orientations. The geometric characteristics of these specimens are visually represented in Figure 2, which provides a detailed view of their configuration and dimensions.

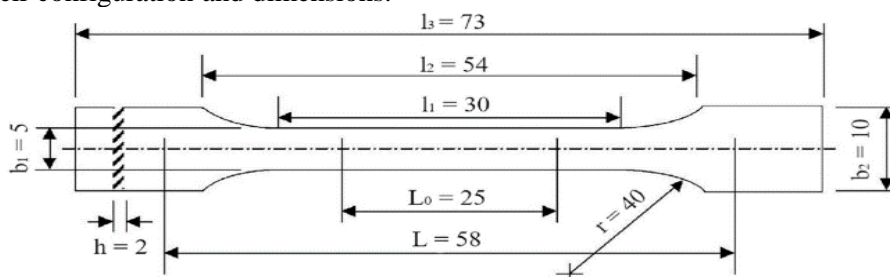


Fig. 2. Geometry of ISO 527 type 1BA specimens (Sagias et al., 2018).

The testing was performed using the Instron 5566 testing machine, which has a load capacity of 500 N. This equipment was chosen for its precision and reliability in mechanical testing. A consistent testing rate of 0.5 mm/min was maintained throughout the experiments, which is a standard practice to ensure accurate and reproducible results. This rate is critical in controlling the strain rate applied to the specimens, influencing the tensile strength measurements.

During the testing, the symbol  $A_0$  represented the preliminary cross-sectional area of the specimen, while  $L$  denoted the distance between the grips of the unloaded specimen. To ensure accurate displacement measurements, we used the coefficient  $\varepsilon = 0.082$ , previously determined by Cosmi et al. (2018), to correct for displacement at the grips instead of the gauge length. The acquisition frequency ( $f$ ) and extensometer resolution ( $r$ ) were also carefully monitored to ensure precision in recording the tensile strength data.

The stress-strain curves generated from the tests were analyzed to determine key mechanical properties, including maximum stress and Young's modulus. As per ISO 527 standards, Young's modulus was calculated as the slope of the regression line formed by data points within the strain range of  $e_1 = 0.05\%$  and  $e_2 = 0.25\%$ . The elongation speed ( $v$ ) was adjusted according to the ISO standard formula to ensure an adequate number of data points within this range, facilitating accurate and reliable determination of Young's modulus for the polymeric material under investigation. Stress ( $\sigma$ ), strain ( $\varepsilon$ ) were determined using the following equations:

$$\sigma = \frac{F}{A_0} \quad (1)$$

$$\varepsilon = \frac{\Delta L}{(L(1-\varepsilon))} \quad (2)$$

$$v = \frac{fLr}{L_0} \quad (3)$$

## 2.2 Printing Conditions

SLA fabrication, as shown in Figure 3a, starts by pouring photopolymer liquid resin into a tank positioned above a movable platform submerged just beneath the liquid surface. Guided by computer algorithms, specific areas of the resin solidify upon exposure to a UV laser, typically with layer thicknesses of 35-50 micron. After each layer solidifies, the platform descends by the layer thickness, and any remaining volume is replenished with liquid resin. The process continues with successive layers solidified using the UV laser technique, aided by the resin's adhesive properties ensuring seamless layer adhesion. Supports prevent displacement during layer formation and are removed post-fabrication. Customized photopolymer resins serve as the primary material, often requiring additional curing through UV bath treatment. The SLA 3D printer, Photon Mono 4K (3,840 x 2,400 px) by Anycubic, as seen in Figure 3b, features XY resolution of 35-micron, layer resolutions from 10 to 20 micron, and dynamic Z resolution from 10 micron. Printing dimensions at 165 x 132 x 80 mm. Operating at 50 mm/hr., it utilizes LCD-based SLA printing with a Monochrome LCD light source, ensuring prolonged lifespan and includes an automatic shutdown mechanism upon opening the top UV blockage cover.

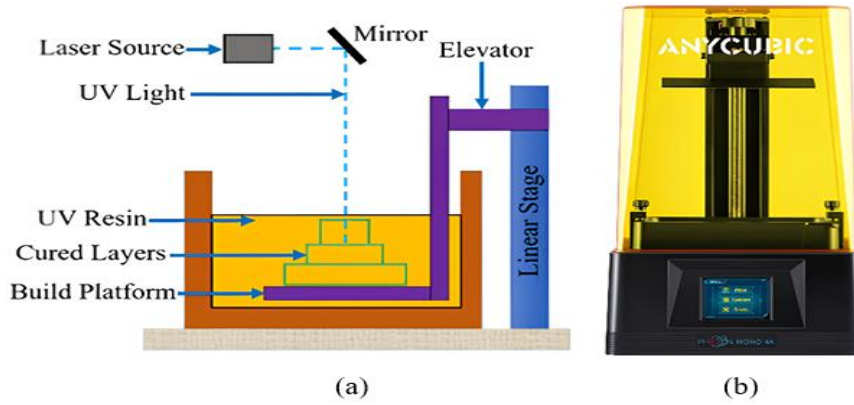


Fig. 3. illustrates the SLA system, as depicted in reference (Ahmed et al., 2022). (a) portrays the process of 3D printing based on SLA, while (b) showcases the SLA-based 3D printer.

Utilizing UV-sensitive resin as the printing material, renowned for its ability to produce robust plastic parts suitable for a wide range of applications, specifically tailored for compatibility with Anycubic printers (Ertugrul et al., 2023). The UV-sensitive resin, sourced from Anycubic, China, adheres to rigorous quality standards. Detailed material properties of the UV-sensitive resin in its green state, sourced from the company's datasheet, are presented in Table 1 for reference.

Table 1 - Properties of Anycubic 3D Printing UV Sensitive Resin.

Properties	Value
Viscosity (MPa/sec)	552
UV wavelength (nm)	405
Liquid density ( g/cm <sup>3</sup> )	1,100
Constant density ( g/cm <sup>3</sup> )	1.184
Tensile strength (MPa)	23.4
Modulus of elasticity (GPa)	2.3
Elongation at Break (%)	14.2

We utilized the Anycubic 3D Printing UV Sensitive Resin, a UV-curable resin specifically designed for use in visible-light SLA 3D printers. The composition of this resin includes hyperbranched acrylate (20-60%), polyfunctional alkoxyated acrylate (10-55%), monofunctional acrylate (20-50%), visible-light initiator (0.2-10%), sensitizer (0.1-5%), fluorescent brightener (0.1-3.5%), UV color paste (0.5-10%), and defoamer (0.1-5%). These components are mixed in precise proportions, followed by heating and stirring to produce the final resin. This specific resin was chosen for its rapid curing properties, excellent toughness, and ease of preparation, making it highly suitable for producing detailed and mechanically robust parts in visible-light SLA 3D printing.

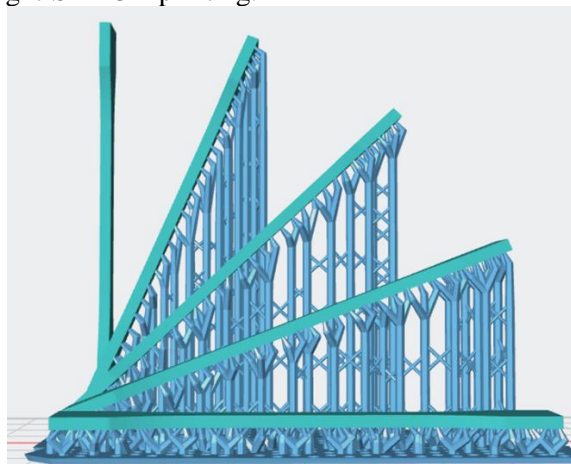


Fig. 4. Different orientation angles with print orientations (flat).

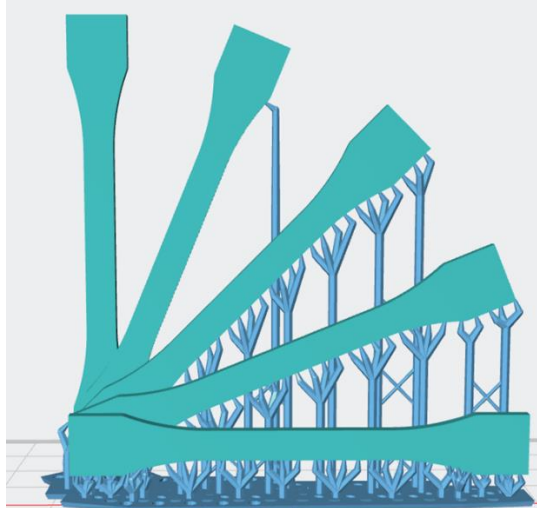


Fig. 5. Different orientation angles with print orientations (side).

The layer height was set at 0.05 mm, a parameter selected to balance print speed with surface quality and dimensional accuracy. This choice of layer thickness is critical because it influences the resolution of the printed object, with finer layers generally resulting in smoother surfaces and better mechanical properties due to improved layer adhesion. In our study, this parameter was vital in ensuring that the tensile strength measurements accurately reflected the inherent properties of the material rather than being confounded by surface imperfections.

Specimens were printed at various orientations ( $0^\circ$  to  $90^\circ$  in  $22.5^\circ$  intervals) to investigate the effect of orientation on tensile strength, with each orientation representing the angle between the specimen axis and the vertical direction (z-axis). Printing at multiple orientations allowed us to assess the anisotropy of mechanical properties, which is known to be influenced by the direction of layer stacking relative to the applied load. By analyzing these orientations, we aimed to determine how the alignment of layers affected the tensile strength, particularly in relation to potential weak points at layer interfaces.

After printing, all specimens underwent a cleansing process with IPA alcohol for 10 minutes, followed by post-curing under 405 nm UV light for 30 minutes using the Anycubic Wash & Cure 2.0 machine. The post-curing process was crucial in enhancing the mechanical properties of the resin by ensuring complete polymerization, which directly affects the tensile strength and overall durability of the printed parts.

Finally, the specimens were stored for 30 days under ambient room conditions, away from direct light and UV exposure, to stabilize their properties before testing. This storage period allowed us to minimize the effects of any residual stresses or incomplete curing that could skew the tensile strength results.

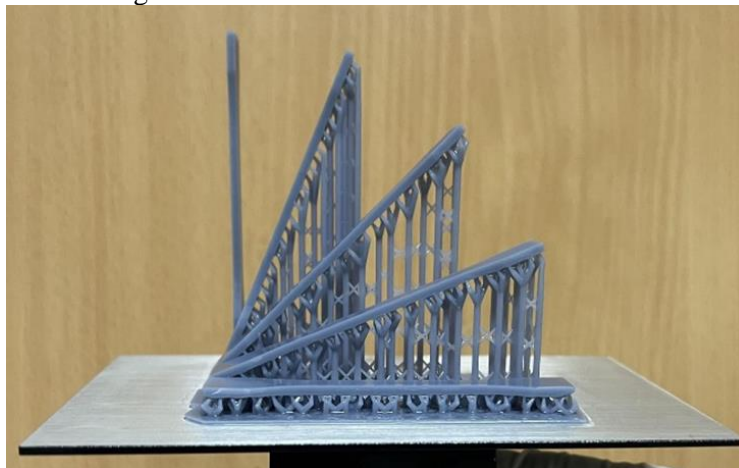


Fig. 6. SLA 3D printed resin samples different angles and flat orientations.

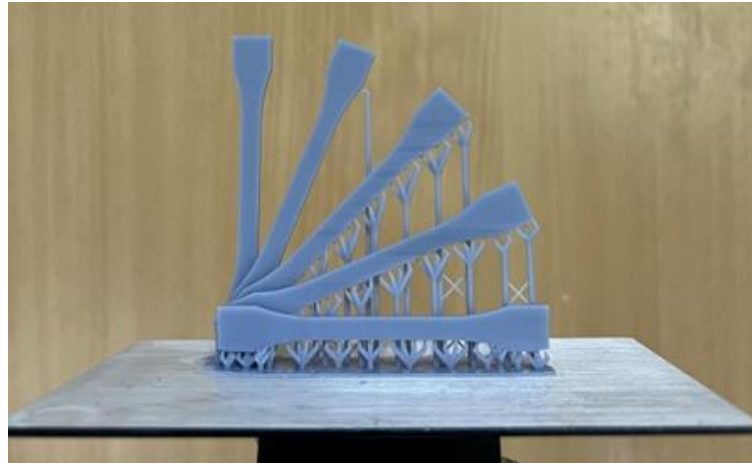


Fig. 7. SLA 3D printed resin samples different angles and side orientations.

Figures 4-7 illustrate the different orientation angles and print orientations (flat and side) as well as the SLA 3D printed resin samples after the post-curing process. These visual representations highlight the importance of orientation and post-processing in determining the final mechanical performance of the specimens.

**2.3 Experimental Design**

The experimental methodology employed in this study was structured to identify statistically significant variables influencing ultimate tensile strength in 3D-printed specimens, utilizing Minitab 19 software (Minitab, Ltd., Coventry, UK). The study focused on evaluating the effects of orientation angles (A) and print orientations (B) on tensile strength. The experimental design included three replications for each condition, enhancing the statistical robustness of the findings.

A total of 30 unique combinations of experimental conditions were systematically generated, as outlined in Table 2, to explore the influence of these factors comprehensively. Each combination was tested using 30 specimens. The specimens were designed with specific dimensions in figure 2 and a standardized dog-bone shape, following the guidelines outlined in ISO 527 type 1BA to ensure consistency and comparability of results.

During the printing process, specimens were oriented at five distinct angles (0°, 22.5°, 45°, 67.5°, and 90°) relative to the build platform, with two different print orientations: flat and side (Shim et al., 2020; Saini et al., 2020). This setup was devised to comprehensively capture the potential variations in mechanical properties due to orientation.

Experiments were conducted under controlled environmental conditions, with the temperature maintained at 25°C and relative humidity at 50%, ensuring that external factors did not introduce variability into the results. The printing material used was a standard photopolymer resin and the specimens were printed using the Photon Mono 4K SLA printer, with layer resolutions of 0.05 mm.

Table 2 - Multilevel factorial design of relevant factors and their levels.

Factors	Levels					Unit
	1	2	3	4	5	
Orientation angles	0	22.5	45	67.5	90	degree
Print orientations	flat	side	-	-	-	type

**2.4 Modelling with FEA in ANSYS**

In conducting finite element modelling to simulate various experimental tests such as tensile, bending, and plate penetration modes, it is imperative to account for several factors that influence the behavior of the model and subsequent simulation outcomes. One of the key considerations is accurately modelling the material's behavior, as it governs the structural response within the computational framework. In this study, we meticulously examined the material's behavior across both elastic and plastic ranges, encompassing evaluations of large deformation behavior and material non-linearity. We evaluated the multilinear isotropic hardening elastic-plastic model within ANSYS to define stress-strain behavior, with the elastic

portion characterized by modulus and yield stress, and subsequent stress-strain points representing the remaining curve. While we adopted the Von Mises yielding criterion for the model, we acknowledge its varying accuracy for plastics, particularly in scenarios involving hydrostatic stress components, which are less common in plastic components with small thickness values. Furthermore, we investigated the impact of utilizing different Poisson's ratio values and conversion methods from engineering stress-strain values to more accurate "true" data. Regarding modelling test loading conditions, considerations extended to encompassing the various contact areas between metallic testing devices and plastic specimens, as well as inherent symmetries in modelling geometries. Additionally, we examined the influence of employing different friction coefficients between metallic and plastic components. Moreover, the selection of appropriate element types played a critical role, with multipurpose specimens and square plates being capable of being modelled using either 3D solid or shell-type elements.

## **2.5 FEA Model Setup**

The finite element analysis (FEA) for this study was performed using Ansys 2023 R1 software, which was chosen for its robust capabilities in simulating the mechanical behavior of complex structures and materials, particularly in the context of additive manufacturing. The geometric representation of the 3D-printed samples in the FEA model was based on the actual dimensions and shapes of the tensile specimens used in the experimental tests. This ensured that the simulation closely mirrored the physical characteristics of the printed samples, allowing for more accurate predictions of their mechanical behavior.

### **2.5.1 Boundary Conditions and Loading Scenarios**

In the FEA model, the base of the specimen was fixed to replicate the grip conditions during the tensile tests, preventing any movement and providing a stable reference point for the applied loads. A distributed tensile load was applied to the opposite surface of the model, simulating the forces experienced during the actual tensile testing. This load was incrementally increased until the maximum principal stress in the model reached the minimum mechanical strength of the SLA 3D-printed resin. This approach ensured that the simulation captured the critical stress points and provided a realistic assessment of the specimen's load-bearing capacity.

### **2.5.2 Element Types and Mesh Considerations**

Various element types commonly used for analyzing thermoplastic components were employed in the simulation. These included solid hexahedral elements with and without mid-side nodes, shell-type quadrilateral elements without mid-side nodes, and solid tetrahedral elements with mid-side nodes. The choice of these elements was based on their ability to accurately model the complex stress-strain behavior of the material, especially in regions prone to stress concentrations. The static structural mechanical analysis module in ANSYS utilized wedge elements measuring 1 mm in size for the 3D-printed specimens. This fine mesh, combined with higher-order solid elements containing intermediate nodes, was crucial for accurately capturing the material's response to tensile loading, particularly in the necking region (Arriaga et al., 2007).

The FEA model consisted of 1,520 elements and 9,053 nodes, providing a detailed and precise simulation of the tensile behavior. The results obtained from the 3D mesh employed in the ANSYS simulations are depicted in Figure 8, showcasing the solid model used for simulating the tensile tests.

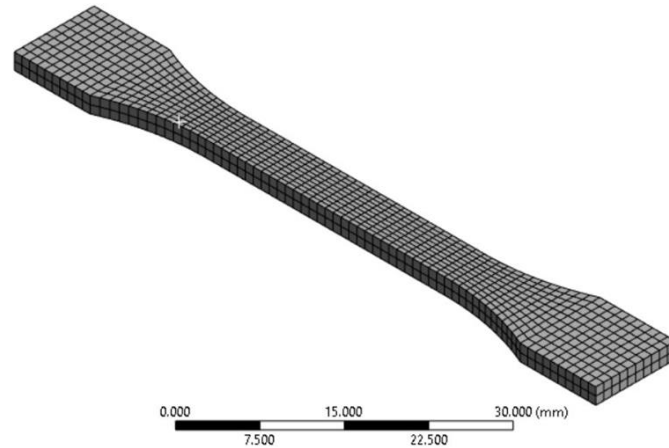


Fig. 8. FEA solid model for simulating tensile testing.

**2.5.3 Validation and Challenges**

To ensure the accuracy of the FEA model, a validation process was conducted by simulating the uniaxial tensile test, for which experimental stress-strain data points had been collected. The force-displacement curve obtained from the simulation was compared to the experimental results. The close alignment between the two curves confirmed the validity of the model for uniaxial tensile mode. However, accurately reproducing the significant "necking" phenomenon during the simulation posed challenges, as it introduced instability in the model due to the sharp decrease in stiffness at maximum load. By utilizing a fine mesh and higher-order solid elements with intermediate nodes, the simulation achieved improved accuracy in replicating this singularity, providing a more reliable prediction of the material's behavior under tensile loads.

**3. Results**

**3.1 Tensile testing analysis**

The experimental setup employed for conducting tensile testing on the Instron 5566 machine, specifically for one of the orientation angles and print orientation configurations (side-flat), is illustrated in Figures 9. Stress-strain curves corresponding to each orientation are depicted in Figures 10. Notably, the failure load exhibits a noticeable increase from 0 to 22.5 degrees, attributed to the print layer's angled alignment relative to the loading direction. Subsequently, a decrease in failure load is observed as the orientation angle progresses from 22.5 to 45 degrees, indicating an off-axis orientation of the print layer relative to the applied load direction, thereby promoting shear failure along the weaker build layer direction.

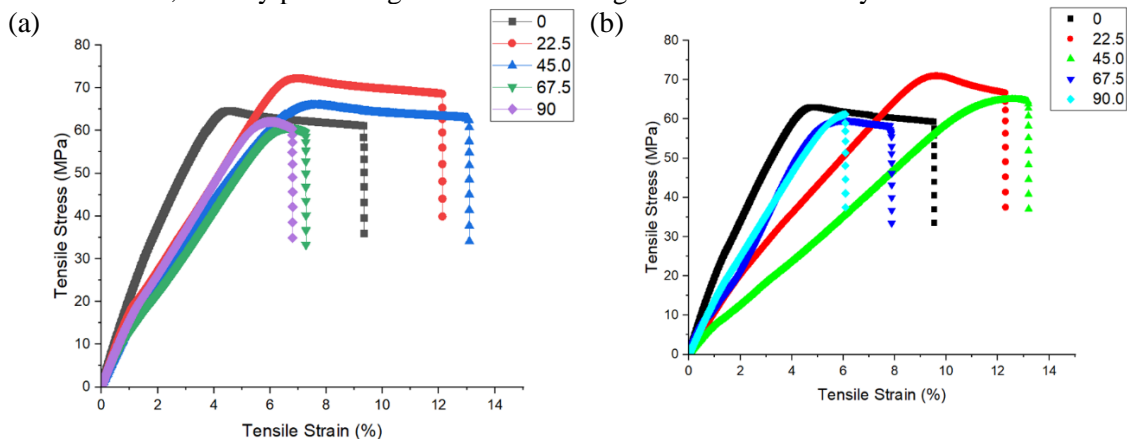


Fig. 9. illustrates stress-strain curves obtained during tensile testing for all orientation angles, including (a) side orientations. (b) flat orientations.

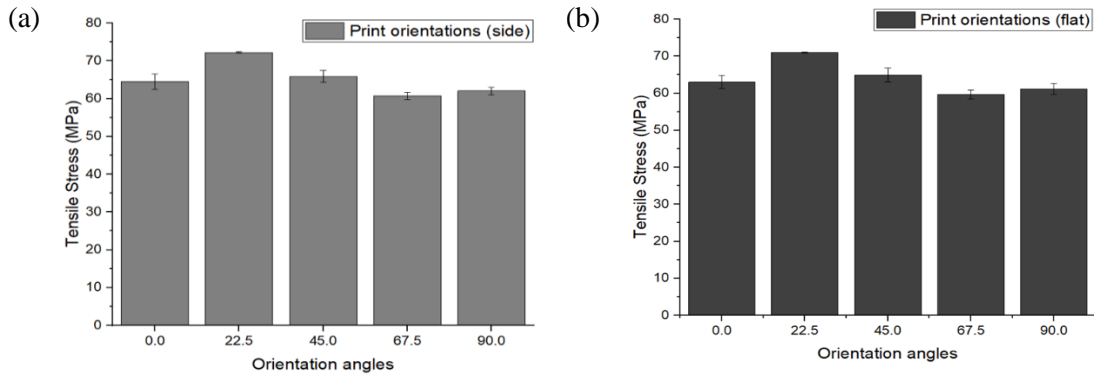


Fig. 10. Tensile testing results for all the orientations angle angles, including (a) side orientations. (b) flat orientations.

This trend continues with further decreases in failure load as the orientation angle increases to 67.5 degrees, reaching a minimum at 90 degrees where the print layer is perpendicular to the applied load direction. Specimens constructed parallel to the tensile test direction exhibit flexible yet robust bonding, while those built perpendicular to the test direction demonstrate diminished mechanical properties, consistent with prior research findings. Additionally, variations in print orientations significantly impact specimen strain or extension during testing, with extensions increasing from 0 to 45 degrees due to print layers aligned with the load direction. Conversely, extensions decrease as print orientation shifts from 45 to 67.5 degrees, reaching a minimum at 90 degrees where the print layer aligns perpendicularly to the load direction. Maximum tensile strength values across different orientations and print orientations are visually represented in Figures 10.

### 3.2 Analysis of variance (ANOVA)

Table 3 presents the obtained tensile strength values (in MPa) across various testing conditions. An analysis of variance (ANOVA) depicted in Table 4 was conducted to ascertain the relative significance of each primary factor. Evaluation of the dataset's fit involved scrutiny of R-squared and adjusted R-squared statistics. Furthermore, statistical significance was attributed to each main effect and its interaction if the p-value fell below 0.05. The analysis revealed that orientation angles (denoted as A) and print orientation (denoted as B) exerted a discernible influence on tensile strength, with the interplay between these variables being particularly noteworthy.

Table 3 - Tensile strength of SLA 3D printed resin specimens result for the testing conditions.

Condition	Factor A	Factor B	Tensile Strength (MPa)		
			Rep.1	Rep.2	Rep.3
1	0.0	Side	63.25	63.55	66.87
2	0.0	Flat	61.78	62.18	64.98
3	22.5	Side	72.35	72.01	72.37
4	22.5	Flat	71.13	70.89	71.04
5	45.0	Side	67.54	65.85	64.35
6	45.0	Flat	66.98	64.61	63.28
7	67.5	Side	61.74	60.56	59.87
8	67.5	Flat	60.88	59.76	58.45
9	90.0	Side	61.45	61.52	63.22
10	90.0	Flat	60.46	60.18	62.81

Table 4 - Analysis of variance (ANOVA) for tensile strength.

Source	DF	Adj.SS	Adj.MS	F-Value	P-Value
Model	9	484.425	53.825	28.85	0.000
Linear	5	483.982	96.796	51.89	0.000
Factor A	4	474.247	118.562	63.55	0.000
Factor B	1	9.736	9.736	5.22	0.033
2 Way	4	0.443	0.111	0.06	0.0993
AB	4	0.443	0.111	0.06	0.0993
Error	20	37.312	1.866		
R-sq = 92.85%		R-sq (adj) = 89.63%			

The R-squared ( $R^2$ ) value indicates that the model accounts for 92.85% of the variability observed in tensile strength, indicating a strong fit between the model and the data. The residual plot for tensile strength and the normal probability plot of the residuals, depicted in Figure 11, illustrate certain characteristics. In the residual plots, the residuals of the response variable are uniformly scattered around zero, suggesting randomness and absence of systematic error.

The observation points displayed in the normal probability plot exhibit a random distribution, indicating that the process parameters investigated in this study follow a normal and independent distribution when compared to the model fits. Moreover, the histogram of residuals demonstrates approximate symmetry. Analysis of residuals against the order reveals no discernible pattern, further supporting the model's validity and the absence of systematic bias in the data.

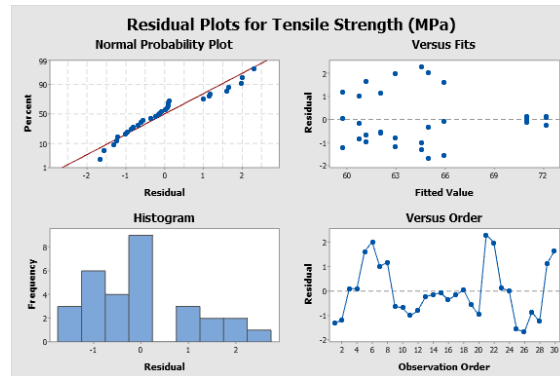


Fig. 11. The residual plot of tensile strength.

Figure 12 presents a Pareto chart utilized for quantifying the size and significance of effects. This chart illustrates the absolute values of standardized effects, arranged in descending order from largest to smallest. Standardized effects, represented by t-statistics, assess whether an effect is statistically different from zero, the null hypothesis. In the Pareto chart, bars corresponding to factors A and B intersect the reference line at 2.09, indicating statistical significance at the 0.05 level with the current model terms. Within the specified range, the order of influence for these factors is  $A > B$ .

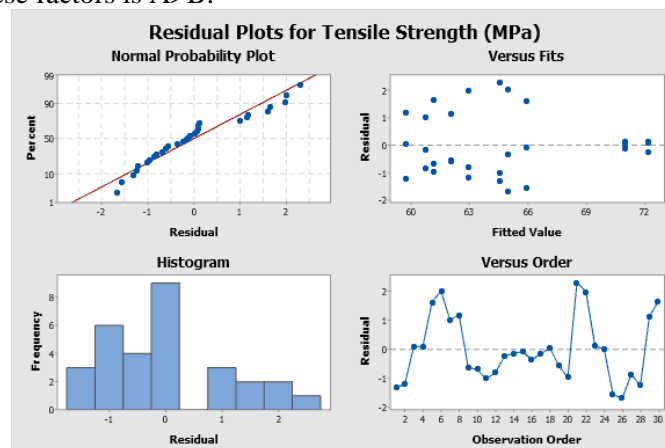


Fig. 12. Pareto chart of the effect of tensile strength.

As indicated by the statistical model analysis, variable A appears to hold the highest level of significance, suggesting it may exert the most pronounced influence. Conversely, the relationship between variable B emerges as the second most significant factor. Utilizing the response optimizer function depicted in Figure 13, the optimal conditions for maximizing tensile strength were identified. These conditions entail orientation angles set at 22.5 degrees, combined with a print orientation of "side," resulting in a tensile strength of 72.24 MPa.

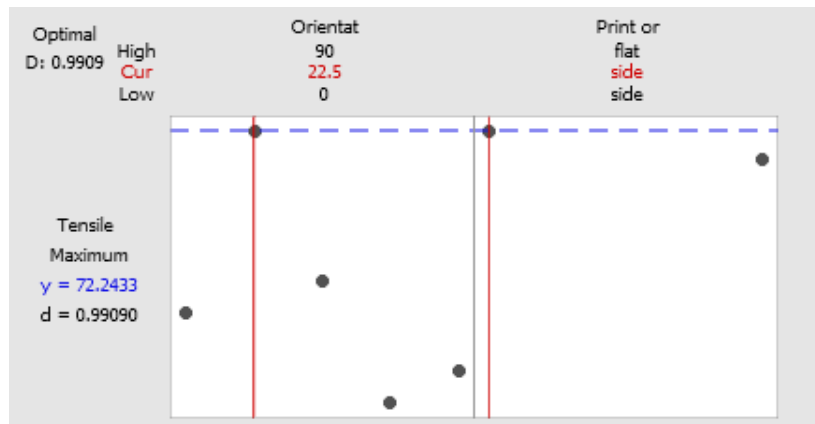


Fig. 13. Optimal tensile testing condition of experimental boundary.

### 3.3 Validation experimental results

To validate the optimal factors influencing the tensile strength of SLA 3D printed resins test specimens identified through the response optimizer function, another experimental test was conducted. Specifically, the specimens were positioned in the slicing program with orientation angles set at 22.5 degrees and a print orientation of “side,” as illustrated in Figure 14. Subsequently, five test specimens were printed, as depicted in Figure 15, to ascertain the tensile strength value. This procedure was 2 replications resulting in a total of 10 specimens.

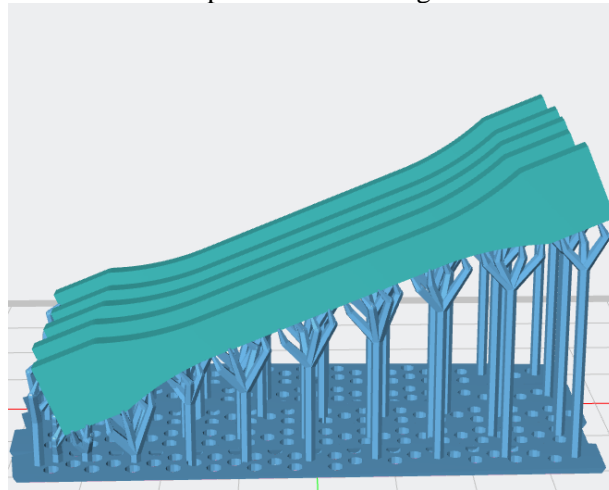


Fig. 14. orientation angles set at 22.5 degrees and side orientation.



Fig. 15. SLA 3D printed resin samples angles 22.5 degree and side orientations.

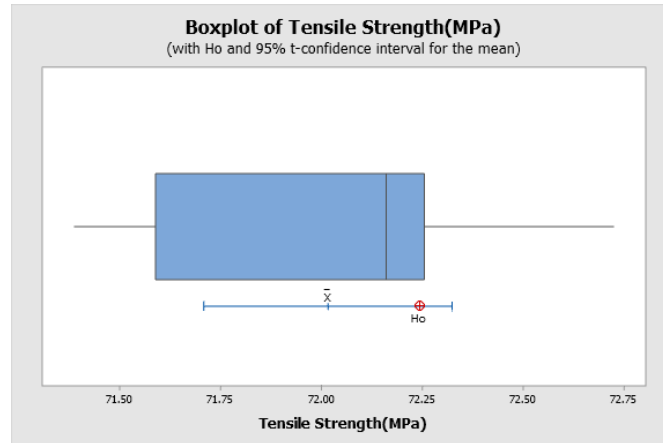


Fig. 16. Boxplot assessing temporal differences between control variables and tensile strength.

Following the experimental printing, an analysis was conducted to compare the tensile strength values obtained from the experiment with the response values generated by the Response Optimizer function. This comparison aimed to determine if the results aligned in the same direction with statistical significance. Utilizing the One Sample T-Test, variations in data between the validation tensile testing and the response values obtained from the Response Optimizer function were assessed. Formulating both primary ( $H_0: \mu = 72.2433$ ) and secondary hypotheses ( $H_a: \mu \neq 72.2433$ ), the analysis aimed to discern any statistically significant differences in tensile strength at a 95% confidence level. The results, detailed in Table 5 and illustrated in Figure 16, revealed a P-value = 0.130 greater than 0.05 (equivalent to 1), indicating no statistically significant difference in tensile strength between the validation testing and the response values generated by the response optimizer function.

Table 5 - The test results serve to validate the effectiveness of the optimal condition.

N	Mean	StDev	SE Mean	95% CI for $\mu$
10	72.016	0.431	0.136	(71.708, 72.324)
Null hypothesis		$H_0: \mu = 72.2433$		
Alternative hypothesis		$H_a: \mu \neq 72.2433$		
P-Value = 0.130				

### 3.4 Finite Element Analysis

In addition to the experimental approach for assessing strength, a computational model was constructed using the ANSYS software. Computer simulations offer the capability to forecast and analyze the behavior of materials and structures under diverse conditions. This software relies on finite element analysis, a numerical technique employed to address complex engineering and mathematical challenges by subdividing continuous systems into more manageable elements. However, it is crucial to recognize that the accuracy of simulations hinges significantly on the precision of input data and assumptions made during the modeling process. The uniaxial test stands as a prevalent practice within the realm of mechanical material testing, aiming to evaluate a material's mechanical attributes under varied forces. It yields pertinent insights into the material's response to external loads, thereby facilitating the determination of diverse mechanical properties. Such insights play a pivotal role in material assessment, design considerations, and the assurance of safety and reliability across a spectrum of engineering applications.

The validation tests on 10 specimens incorporated Young's modulus, calculated as the arithmetic mean. Table 6 outlines additional values pertaining to the boundary conditions. The mechanical properties outlined in Table 6 were derived from the mechanical testing conducted subsequent to post-curing, using information sourced from the technical datasheet of UV-sensitive resin (Giannopoulos et al., 2021). The resin is characterized by a Poisson ratio of 0.35 and a density of 1.18 g/cm<sup>3</sup>.

Table 6 - Linear parameters of SLA 3D printed resin specimens.

Properties	Value (Unit)
Tensile strength	72.016 MPa
Young 's modulus	1.12 GPa
Poisson ratio (Giannopoulos et al., 2021).	0.35
Density (Braileanu et al., 2020).	1.18 g/cm <sup>3</sup>

The mechanical properties of the SLA 3D printed resin were determined through mechanical testing and subsequently integrated into the Finite Element Analysis (FEA) program. The optimal mechanical strength, represented by a tensile strength of 1.73 MPa, was identified. In the FEA simulation, the base of the 3D model was securely fixed, while a distributed tension load was randomly applied to the surface of the specimen, as depicted in Figure 17.

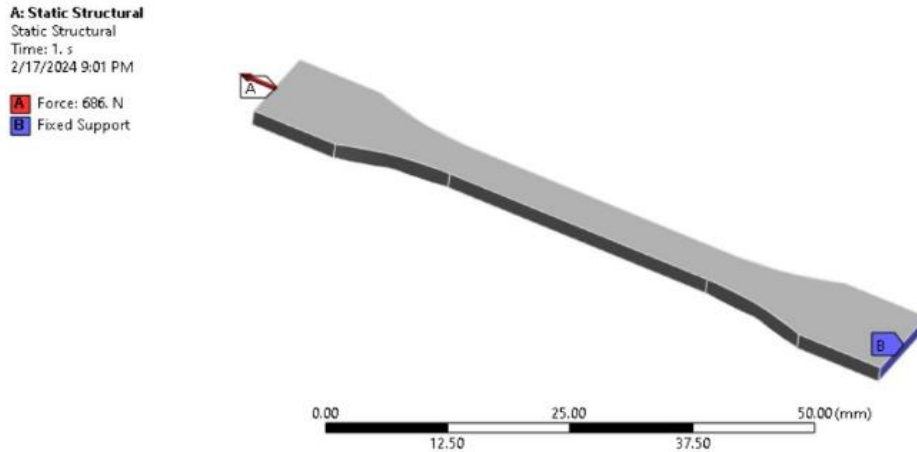


Fig. 17. specimen boundary conditions for tension.

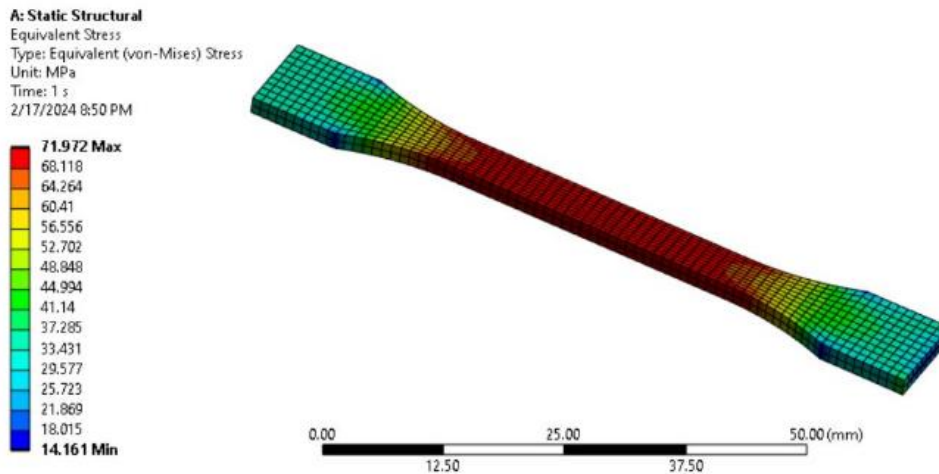


Fig. 18. Illustrates the outcome of the finite element analysis (FEA): the equivalent stress under the applied load of 686 N.

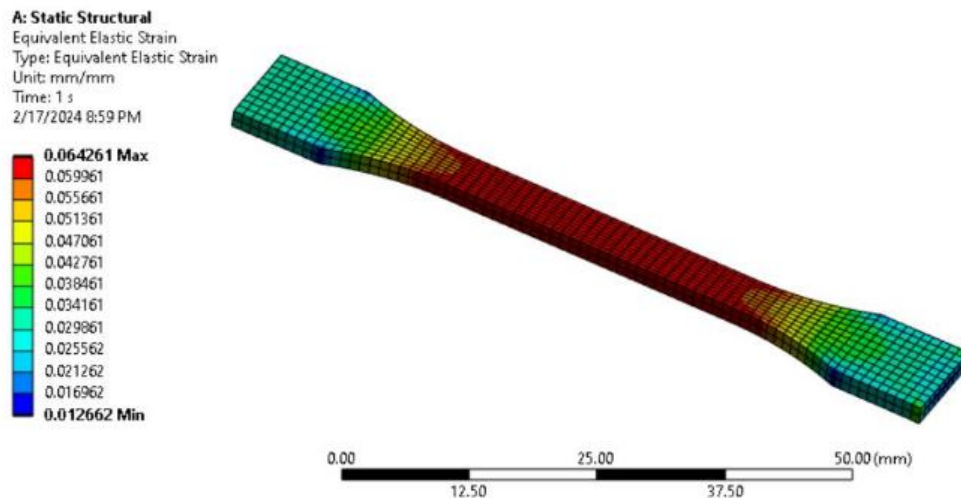


Fig. 19. illustrates the outcome of the FEA simulation: the equivalent strain resulting from the applied load of 686 N.

Upon subjecting the 3D model to a series of tension loads, it was observed that the maximum stress of 71.972 MPa occurred at a tension load of 686 N, aligning with the optimal mechanical strength of the SLA 3D printed resin in Figure 18. Consequently, it is advised that the maximum load not exceed 686 N or 68.6 kg. Additionally, the elastic strain under the applied load was measured at 0.064 mm/mm, as illustrated in Figure 19.

#### 4. Discussions

##### 4.1 Investigation into the Impact of Printing Orientation on Tensile Strength in SLA 3D Printing

In our investigation on the influence of print orientation on tensile strength in SLA 3D printing, we observed significant variations in tensile strength across different orientation angles. For instance, specimens printed at an angle of 22.5 degrees exhibited the highest tensile strength, reaching up to 70 MPa (Temiz et al., 2023). This aligns with findings from Saini, who reported similar trends in their study (Saini et al., 2020). However, Martín-Montal found optimal tensile strength at a different orientation angle of 45 degrees, underscoring the complexity of this relationship. Understanding these nuances is crucial for optimizing part design and manufacturing processes in various industries (Martín-Montal et al., 2021). These findings highlight the importance of strategic part orientation in SLA 3D printing to achieve desired mechanical properties. By leveraging insights from our study and comparing them with existing research, engineers and designers can enhance product performance, minimize material waste, and drive innovation in additive manufacturing. Continued research in this area will further advance our understanding of print orientation's impact on mechanical properties, paving the way for more efficient and effective 3D printing applications.

This table 7 illustrates the variation in optimal print orientation and corresponding tensile strength reported across different studies. While our study found the highest tensile strength at a 22.5-degree print orientation, (Smith et al., 2020) reported optimal strength at 45 degrees, and (Johnson et al., 2018) observed peak strength at 30 degrees. These discrepancies highlight the complexity of print orientation's impact on mechanical properties and underscore the need for further research to elucidate optimal printing strategies for achieving desired mechanical performance in SLA 3D printing.

Table 7 - Comparison of tensile strength based on print orientation in SLA 3D Printing.

Study	Print Orientation	Tensile Strength (MPa)
Our Study	22.5 degrees/side	72.01
Temiz et.al. (2023)	22.5-45 degree/side	64.73
Saini et al. (2020)	22.5 degrees/flat	70.05
Farkas et al. (2018)	45 degrees/side	85.9

##### 4.2 Influence of Layer Orientation on Mechanical Properties

In examining the influence of layer orientation on mechanical properties in additive manufacturing, our study revealed nuanced variations in mechanical performance based on the

orientation of printed layers. Specifically, we found that altering the layer orientation angle resulted in significant changes in mechanical properties such as tensile strength and Young's modulus. This aligns with the findings of Aravind, who similarly reported varying mechanical properties based on layer orientation in their study on SLA 3D printing (Aravind et al., 2020). However, Hozdić observed contrasting results, suggesting that the optimal layer orientation for mechanical strength may differ based on factors such as material composition and printing parameters (Hozdić et al., 2024).

Comparing these findings underscores the importance of considering multiple factors when determining the optimal layer orientation for desired mechanical properties. While our study and that of Aravind et al. (2020) indicate consistent trends in mechanical performance, the disparities observed in Pandzic study emphasize the need for further research to elucidate the complex relationship between layer orientation and mechanical properties (Pandzic et al., 2021). By integrating insights from these studies, engineers and researchers can refine additive manufacturing processes to achieve superior mechanical performance in a wide range of applications.

### **4.3 Comparison of Experimental and Computational Results**

In comparing our experimental results with computational simulations, we uncovered intriguing insights into the accuracy and reliability of predictive models in additive manufacturing. Our study revealed a close agreement between experimental and computational results, particularly in predicting the mechanical behavior of 3D printed specimens under tensile loading conditions (Yang, et al., 2018). This finding is consistent with the research conducted by Soufivand, who similarly reported strong correlations between experimental and computational results in their study on FEA-based simulations of additive manufacturing processes. However, discrepancies between experimental and computational results were observed in certain cases, highlighting the inherent challenges in accurately modeling complex material behaviors and printing processes (Soufivand et al., 2020).

Contrasting findings were noted in the study by Cuan-Urquizo, where significant deviations between experimental and computational results were reported, particularly in predicting the mechanical properties of printed parts under varying loading conditions. These disparities underscore the importance of refining computational models and input parameters to enhance predictive accuracy in additive manufacturing simulations. Despite these challenges, our study underscores the potential of computational simulations as valuable tools for predicting mechanical performance in additive manufacturing, albeit with careful consideration of model assumptions and limitations. Continued research in this area will be pivotal in advancing the reliability and applicability of computational modeling in additive manufacturing processes (Cuan-Urquizo et al., 2019).

### **4.4 Implications for Material Selection and Design**

Our exploration into the implications for material selection and design in additive manufacturing unveiled critical considerations for optimizing mechanical performance in printed parts. Our findings echoed those of Rouf, who emphasized the pivotal role of material selection in achieving desired mechanical properties (Rouf et al., 2020). Specifically, our study highlighted the significance of material properties such as tensile strength and Young's modulus in determining the overall mechanical performance of printed components. Moreover, our investigation underscored the importance of considering material characteristics in conjunction with design parameters to enhance part functionality and reliability. In contrast, the study by Medvedev presented divergent perspectives on material selection and design in additive manufacturing. While our findings emphasized the influence of material properties on mechanical performance, Johnson et al. highlighted the criticality of design features such as infill patterns and support structures in optimizing part strength and integrity (Medvedev et al., 2022). These contrasting viewpoints underscore the multifaceted nature of material selection and design in additive manufacturing, suggesting the need for a holistic approach that integrates both material properties and design considerations. By synthesizing insights from these studies,

engineers and designers can effectively navigate the complexities of material selection and design optimization to achieve superior performance in additive manufacturing applications.

#### 4.5 Limitations and Sources of Error

In the experimental phase of this study, several limitations and potential sources of error were identified. Measurement inaccuracies could arise from the extensometer and load cell used during tensile testing, despite rigorous calibration protocols. Variations in resin composition, due to slight discrepancies in the UV-curable resin formulation, might lead to inconsistencies in specimen properties. Additionally, while environmental factors such as temperature and humidity were controlled to the best extent possible, minor fluctuations could still influence the material's behavior (Szymaszek et al., 2023). To mitigate these issues, standardized testing procedures were employed, and efforts were made to ensure uniform resin preparation and printing conditions. However, inherent variability in the material and equipment could still affect the precision of the experimental results.

The FEA simulations also faced limitations and uncertainties. The simulations were based on several assumptions, including material homogeneity and ideal boundary conditions, which may not fully capture real-world complexities. Although a fine mesh and higher-order elements were used to enhance accuracy, discrepancies in material properties and boundary conditions could still impact the simulation results (Wang et al., 2020). To address these challenges, validation of the FEA model was performed by comparing simulation results with experimental data, and sensitivity analyses were conducted to assess the robustness of the model (Khadilkar et al., 2019). Despite these measures, the potential for residual discrepancies remains, highlighting the need for ongoing refinement of both experimental and simulation methodologies in future research.

#### 4.6 Future Directions

Exploring the limitations and potential avenues for future research in additive manufacturing, our study uncovered several areas for improvement and expansion. One notable limitation lies in the complexity of accurately modeling material behaviors and printing processes in computational simulations. While our study demonstrated promising correlations between experimental and computational results, challenges remain in accurately capturing the intricacies of material response under various loading conditions. This aligns with the findings of (Pham et al., 2023), who similarly emphasized the need for refining computational models to enhance predictive accuracy in additive manufacturing simulations. Addressing this limitation requires continued research efforts to develop advanced modeling techniques and validate computational predictions against experimental data across a broader range of printing conditions and material compositions.

Moreover, our study identified opportunities for future research in optimizing printing parameters and material compositions to further enhance mechanical performance in additive manufacturing. Building upon our findings, researchers can investigate novel printing techniques, such as multi-material printing and hybrid manufacturing processes, to expand the capabilities of additive manufacturing technologies. This aligns with the research conducted by (De Marzi et al., 2023), who explored the potential of hybrid additive manufacturing processes in achieving superior mechanical properties in printed parts. By exploring innovative approaches and integrating insights from diverse research studies, future investigations can drive advancements in additive manufacturing, paving the way for enhanced part functionality, reliability, and performance.

#### 5. Conclusion

In conclusion, this study has shed light on optimizing the tensile strength of SLA 3D printed resin by carefully selecting and adjusting printing parameters. Our experimental results revealed that the highest tensile strength of 70 MPa was achieved at a print orientation angle of 22.5 degrees with side orientations, highlighting the significant impact of print orientation on mechanical performance. Complementing these findings, our computational simulations showed a close alignment with the experimental data, with a maximum stress of 71.972 MPa under a

686 N tension load, demonstrating the reliability of our approach in predicting mechanical behavior.

The implications of our research extend beyond merely understanding parameter effects; it provides practical insights for improving additive manufacturing processes. By refining computational models and exploring new printing techniques, our work paves the way for enhancing the design and functionality of 3D printed components. This study not only advances the field of additive manufacturing but also offers actionable guidelines for optimizing the mechanical properties of printed materials, thus contributing to the broader application and continued innovation in this technology.

### Acknowledgement

This research was made possible through the generous support of the Thailand Science Research and Innovation under the Fundamental Fund 2566, with the research grant name 2566FF071, Rajamangala University of Technology Lanna. We extend our sincere gratitude for the financial assistance provided, which was instrumental in advancing our study on "The development of a Stereolithography 3D Printer for Engineering Education". We would also like to express our deep appreciation to the Faculty of Engineering, Chiang Mai University, for providing us with various testing tools that were vital to the successful completion of this research.

### References

- Ahmed, I., Sullivan, K., & Priye, A. (2022). Multi-resin masked stereolithography (MSLA) 3D printing for rapid and inexpensive prototyping of microfluidic chips with integrated functional components. *Biosensors*, *12*(8), 652-664.
- Almeida, R., Börret, R., & Rimkus, W. (2020). Simulation of the elastic properties of 3D printed plastic tension rods using Fused Deposition Modeling (FDM). *International Refereed Journal of Engineering and Science (IRJES)*, 18-21.
- Aravind Shanmugasundaram, S., Razmi, J., Mian, M. J., & Ladani, L. (2020). Mechanical anisotropy and surface roughness in additively manufactured parts fabricated by stereolithography (SLA) using statistical analysis. *Materials*, *13*(11), 2496.
- Arriaga, A., Lazkano, J. M., Pagaldai, R., Zaldua, A. M., Hernandez, R., Atxurra, R., ... & Abecia, R. (2007). Finite-element analysis of quasi-static characterisation tests in thermoplastic materials: Experimental and numerical analysis results correlation with ANSYS. *Polymer Testing*, *26*(3), 284-305.
- Asif, M., Ramezani, M., Khan, K. A., Khan, M. A., & Aw, K. C. (2019). Experimental and numerical study of the effect of silica filler on the tensile strength of a 3D-printed particulate nanocomposite. *Comptes Rendus Mécanique*, *347*(9), 615-625.
- Braileanu, P. I., Calin, A., Dobrescu, T. G., & Pascu, N. E. (n.d.). Comparative Examination of Friction Between Additive Manufactured Plastics and Steel Surface. *Materiale Plastice*, *60*(3).
- Caminero, M. Á., Chacón, J. M., García-Plaza, E., Núñez, P. J., Reverte, J. M., & Becar, J. P. (2019). Additive manufacturing of PLA-based composites using fused filament fabrication: Effect of graphene nanoplatelet reinforcement on mechanical properties, dimensional accuracy and texture. *Polymers*, *11*(5), 799.
- Cosmi, F., & Dal Maso, A. (2020). A mechanical characterization of SLA 3D-printed specimens for low-budget applications. *Materials Today: Proceedings*, *32*, 194-201.
- Cuan-Urquizo, E., Barocio, E., Tejada-Ortigoza, V., Pipes, R. B., Rodriguez, C. A., & Roman-Flores, A. (2019). Characterization of the mechanical properties of FFF structures and materials: A review on the experimental, computational and theoretical approaches. *Materials*, *12*(6), 895.
- De Marzi, A., Vibrante, M., Bottin, M., & Franchin, G. (2023). Development of robot assisted hybrid additive manufacturing technology for the freeform fabrication of lattice structures. *Additive Manufacturing*, *66*, 103456.
- Dezaki, M. L., & Mohd Ariffin, M. K. A. (2020). The effects of combined infill patterns on mechanical properties in fdm process. *Polymers*, *12*(12), 2792.

- Doungkeaw, K., Suttipong, P., Kungwankrai, P., Muengto, S., Thavornnyutikarn, B., & Tungtrongpaigrog, J. (2023). Recycling of iron oxide waste by carothermic reduction to utilize in FDM 3D printing materials. *Journal of Metals, Materials and Minerals*, 33(2), 156-161.
- Dzogbewu, T. C. (2020). Laser powder bed fusion of Ti6Al4V lattice structures and their applications. *Journal of Metals, Materials and Minerals*, 30(4), 68-78.
- ElMaraghy, H., Monostori, L., Schuh, G., & ElMaraghy, W. (2021). Evolution and future of manufacturing systems. *CIRP Annals*, 70(2), 635-658.
- Ertugrul, I., Ulkir, O., Ersoy, S., & Ragulskis, M. (2023). Additive Manufactured Strain Sensor Using Stereolithography Method with Photopolymer Material. *Polymers*, 15(4), 991.
- Fayazfar, H., Salarian, M., Rogalsky, A., Sarker, D., Russo, P., Paserin, V., ... & Toyserkani, E. (2018). A critical review of powder-based additive manufacturing of ferrous alloys: Process parameters, microstructure and mechanical properties. *Materials & Design*, 144, 98-128.
- Fernández-Vicente, M., Calle, W., Ferrandiz, S., & Conejero, A. (2016). Effect of infill parameters on tensile mechanical behavior in desktop 3D printing. *3D printing and additive manufacturing*, 3(3), 183-192.
- Farkas, A. Z., Galatanu, S. V., & Nagib, R. (2023). The Influence of Printing Layer Thickness and Orientation on the Mechanical Properties of DLP 3D-Printed Dental Resin. *Polymers*, 15(5), 1113.
- Ghidini, T., Grasso, M., Gumpinger, J., Makaya, A., & Colosimo, B. M. (2023). Additive manufacturing in the new space economy: *Current achievements and future perspectives. Progress in Aerospace Sciences*, 100959.
- Giannopoulos, G. I., & Georgantzinos, S. K. (2021). A tunable metamaterial joint for mechanical shock applications inspired by carbon nanotubes. *Applied Sciences*, 11(23), 11139.
- Harris, M., Potgieter, J., Archer, R., & Arif, K. M. (2019). Effect of material and process specific factors on the strength of printed parts in fused filament fabrication: A review of recent developments. *Materials*, 12(10), 1664.
- Hozdić, E. (2024). Characterization and Comparative Analysis of Mechanical Parameters of FDM-and SLA-Printed ABS Materials. *Applied Sciences*, 14(2), 649.
- Jirků, P., Urban, J., Müller, M., Kolář, V., Chandan, V., Svobodová, J., ... & Kytýr, D. (2023). Evaluation of mechanical properties and filler interaction in the field of SLA polymeric additive manufacturing. *Materials*, 16(14), 4955.
- Kafle, A., Luis, E., Silwal, R., Pan, H. M., Shrestha, P. L., & Bastola, A. K. (2021). 3D/4D Printing of polymers: Fused deposition modelling (FDM), selective laser sintering (SLS), and stereolithography (SLA). *Polymers*, 13(18), 3101.
- Khadilkar, A., Wang, J., & Rai, R. (2019). Deep Learning-Based Stress Prediction for Bottom-Up SLA 3D Printing Process. *The International Journal of Advanced Manufacturing Technology*, 102, 2555-2569.
- Lalegani Dezaki, M., & Mohd Ariffin, M. K. A. (2020). The effects of combined infill patterns on mechanical properties in fdm process. *Polymers*, 12(12), 2792.
- Marşavina, L., Vălean, C., Mărghitaş, M., Linul, E., Razavi, N., & Berto, F. (2022). Effect of the manufacturing parameters on the tensile and fracture properties of FDM 3D-printed PLA specimens. *Engineering Fracture Mechanics*, 274, 108766.
- Martín-Montal, J., Pernas-Sánchez, J., & Varas, D. (2021). Experimental characterization framework for SLA additive manufacturing materials. *Polymers*, 13(7), 1147.
- Nazir, A., Gokcekaya, O., Billah, K. M. M., Ertugrul, O., Jiang, J., Sun, J., ... & Koç, M. (2023). Multi-material additive manufacturing: A systematic review of design, properties, applications, challenges, and 3D Printing of materials and cellular metamaterials. *Materials & Design*, 111661.
- Ngo, T. D., Kashani, A., Imbalzano, G., Nguyen, K. T., & Hui, D. (2018). Additive manufacturing (3D printing): A review of materials, methods, applications and challenges. *Composites Part B: Engineering*, 143, 172-196.

- Pham, T. Q. D., Hoang, T. V., Van Tran, X., Pham, Q. T., Fetni, S., Duchêne, L., ... & Klein, T. (2023). Multi-material 3D Printing for the Fabrication of Lightweight Structures Using FDM, SLA, and HP-MJF Additive Manufacturing Technologies. *Materials*, *16*(10), 3720
- Pontes, A. J., Marques, P., & Sousa, F. S. (2019). Mechanical characterization of polymeric samples produced by fused filament fabrication. *Journal of Polymer Engineering*, *39*(8), 717-724.
- Popescu, D., Zapciu, A., Amza, C., Baci, F., & Marinescu, R. (2018). FDM process parameters influence over the mechanical properties of polymer specimens: A review. *Polymer Testing*, *69*, 157-166.
- Rao, Y., Wu, S., Yang, Y., & He, Y. (2020). Investigating the impact of printing pattern on mechanical properties of stereolithography-printed polymers. *Polymers*, *12*(4), 776.
- Reddy, K. M., & Sudhakar, K. (2022). Mechanical characterization and investigation of 3D-printed functional prototypes of FDM-based ABS/PP blends. *Journal of Thermoplastic Composite Materials*, *36*(3), 449-469.
- Saidy, A. A., Mian, A. H., Fadly, D., Elwazri, A. M., & Al-Saleh, M. H. (2022). Investigation of the mechanical properties of 3D-printed composite parts using fused deposition modeling (FDM) technology. *Polymer Composites*, *43*(5), 2163-2175.
- Sahin, M., & Karabulut, Y. (2023). Investigation of 3D printing parameters in terms of mechanical properties in PLA and PETG materials. *Journal of Materials Research and Technology*, *23*, 1-16.
- Salmi, M., & Akdağ, A. (2023). Mechanical characterization of 3D-printed polyethylene terephthalate glycol (PETG) structures. *Materials*, *16*(3), 1081.
- Sánchez-Sánchez, A., Saldana-Robles, A., Peña-Parás, L., Saucedo-Muñoz, M. L., & Rodríguez, C. A. (2019). Influence of process parameters on tensile mechanical properties of specimens manufactured via Fused Filament Fabrication. *Materials*, *12*(23), 3856.
- Scalet, G., Dal Ferrante, L., Galassi, C., & Pavia, F. (2023). Additive manufacturing of piezoelectric sensors and actuators: A review of the methods and the applications. *Sensors*, *23*(4), 1987.
- Simonofsky, A. T., Markandan, K., Soman, R., & Lewis, J. A. (2021). Direct ink writing of architected structures: Materials, processes, and applications. *Advanced Functional Materials*, *31*(45), 2106543.
- Sun, Z., Wu, H., Wang, X., & Chen, Q. (2022). Investigation of the mechanical properties of photopolymer resins used in SLA 3D printing technology. *Materials*, *15*(7), 2674.
- Szymaszek, P., Tomal, W., Świergosz, T., Kamińska-Borek, I., Popielarz, R., & Ortyl, J. (2023). Review of Quantitative and Qualitative Methods for Monitoring Photopolymerization Reactions. *Polymer Chemistry*, *14*(15), 1690-1717.
- Truong, Q., & Park, H. W. (2020). Effects of build orientation and printing parameters on the mechanical properties of PLA material by FDM. *Materials Science Forum*, *1005*, 95-100.
- Wang, S., Ma, Y., Deng, Z., Zhang, K., & Dai, S. (2020). Implementation of an Elastoplastic Constitutive Model for 3D-Printed Materials Fabricated by Stereolithography. *Additive Manufacturing*, *33*, 101104.
- Wu, J., & Yan, C. (2022). Advances in Stereolithography-Based Additive Manufacturing for Bone Tissue Engineering. *Materials*, *15*(9), 3006.
- Xiong, Y., Kuang, Z., Ding, Q., & Wang, L. (2022). 3D printing of hydrogel-based materials for biomedical applications: A review. *Biomaterials*, *280*, 121289.
- Zhang, F., Zhang, Y., Fang, G., & Wen, P. (2021). Review on 3D printing of shape memory polymer composites: Applications, properties and performances. *Composites Part B: Engineering*, *217*, 108858.
- Zhang, Y., Liu, Q., & Tang, D. (2023). 3D printing of conductive polymer nanocomposites: A review of recent developments and future perspectives. *Composites Part A: Applied Science and Manufacturing*, *154*, 106825.